

# Statistical Mechanics of Unperturbed Polypropylene Chains. Analysis of Nuclear Magnetic Resonance Proton Coupling Constants

S. Brückner, L. Malpezzi Giunchi, and G. Allegra\*

Istituto di Chimica del Politecnico, 20133 Milano, Italy. Received July 31, 1979

**ABSTRACT:** Comparison between observed and calculated values of the vicinal proton coupling constants for both iso- and syndiotactic polypropylenes suggests that the nonbonded interactions between atoms separated by more than four C-C bonds should be taken into account, at least as a mean effect. This conclusion is also supported by calculations that indicate the average effect due to the above interactions is of the order of a few kcal/mol for some conformations otherwise having a relatively low energy content. In the present paper such an effect is simulated by attributing a particularly large size to the skeletal atoms when they interact with each other under a separation of four bonds. At the same time the size of the methyl group is reduced with respect to earlier calculations (G. Allegra and S. Brückner, *Macromolecules*, **10**, 106 (1977)) in order to reproduce more closely the observed gauche/trans energy difference of butane. The calculated coupling constants are in satisfactory agreement with experiment. Furthermore, although the trans skeletal rotations are more favored with respect to the gauche ones than before, the methyl size reduction leads to fewer restrictions in the sequence of the rotation angles. As a consequence, the overall chain flexibility is not appreciably changed and the calculated characteristic ratios for polypropylenes of varying tacticity at least maintain the same satisfactory agreement with  $\Theta$ -solution experiments as did the results reported in the above-quoted paper. The double-Fourier expansion method giving the full configurational integral, together with the pseudostereochemical equilibrium approach, was used to obtain the unperturbed dimensions of polymers with different statistical distributions of  $d$  and  $l$  monomer units, as in the above-quoted paper. For reasons of numerical accuracy, the probabilities of the skeletal rotation angles were calculated by iterative multiplication of correlation matrices obtained by sampling the energy maps at intervals of  $10^\circ$  along each angle.

To the best of our knowledge little attention has been paid hitherto to the conformational interpretation of the NMR coupling constants  $H_0 \cdots H_1$  ( $J_{01}$ ) and  $H_0 \cdots H_2$  ( $J_{02}$ ) (Figure 1) in iso- and syndiotactic polypropylenes. Perhaps the most detailed analysis was carried out in 1968 by Zambelli, Giongo, and Natta,<sup>1</sup> who showed from a semi-quantitative viewpoint that the coupling constants are consistent with the cis opening of the double bond during the stereospecific polymerization of either type. We have thought it useful to reexamine this problem from a more detailed statistical-conformational point of view.

In two previous papers, two of us investigated the chain statistics of unperturbed polypropylenes having different steric structures covering the whole field from perfect isotactic, through atactic with various degrees of randomness, to perfect syndiotactic.<sup>2,3</sup> The whole continuum of rotational states was considered within the interdependent rotation scheme, and the random chain structure was treated within the pseudostereochemical equilibrium approach.<sup>3</sup> Our principal objective was to evaluate the characteristic ratios as well as their temperature coefficients and to compare the results with experiment; the agreement appeared to be satisfactory. In particular, in accordance with Boyd and Breitling,<sup>4</sup> it was shown that the relatively small experimental value of  $C_\infty$  for isotactic polypropylene could be accounted for within the usual nonbonded interaction scheme with interdependent rotations. No assumption of steric defects in a proportion greater than 1-2% was necessary, in agreement with the experimental results obtained by Zambelli and co-workers.<sup>5</sup> This view was later supported by detailed calculations carried out by Suter and Flory.<sup>6</sup>

Our previous conformational analysis was based on two specific assumptions<sup>2,3</sup> within the current framework of polymer molecular mechanics.<sup>7</sup> First of all, each methyl group was treated as a spherically symmetrical body, i.e., as a pseudoatom with a suitable size and softness to account for its several degrees of geometrical freedom (i.e., rotation around the C-CH<sub>3</sub> bond in addition to C-C-H and H-C-H bond angle strain). Second, the interactions

involving two skeletal atoms four bonds apart were treated as if due to a pair of methyl groups, to account roughly for the steric repulsion between their pendant atoms. (It should be noted that interactions between atoms separated by more than four bonds cannot be explicitly accounted for unless correlation maps depending on more than two rotation angles are utilized, contrary to current practice as well as expediency.) However, subsequent calculations showed that, in spite of the satisfactory results obtained for the unperturbed dimensions, the above energy maps did not produce values of the proton coupling constants  $J_{01}$  and  $J_{02}$  in acceptable agreement with experiment. It became also clear that, if the interactions between skeletal atoms four bonds apart were made stronger by increasing the repulsive term (i.e., expanding the size of the pseudoatoms), the results of  $J_{0k}$  ( $k = 1, 2$ ) consistently improved for both the iso- and syndiotactic polymers. It seemed a natural conclusion that the *effective* repulsion between skeletal atoms separated by four bonds was in fact larger than that between two methyl groups and that the reason for the increased repulsion should reside in the bulkiness of their pendant atoms, not all of which are hydrogens. We postpone a quantitative discussion to the next section, where the importance of this effect is proven. Here we simply characterize the present study as a new investigation of the configurational properties of polypropylene with different tacticity (i.e., ranging from the isotactic to the syndiotactic polymer), the qualifying points of which are: (i) all possible rotational states are accounted for and (ii) interactions between skeletal C atoms separated by four bonds are treated as involving pseudoatoms with a size larger than that of the methyl groups. Although the principal scope of the present study is to provide a theoretical interpretation of the experimentally observed coupling constants  $J_{0k}$  for the two stereoregular polypropylenes, the assumption of two different size parameters for the pseudoatoms obviously requires additional experimental information to be fitted. The additional experimental facts are: (1) the characteristic ratios of polypropylenes with different tacticity (Table II) and (2)

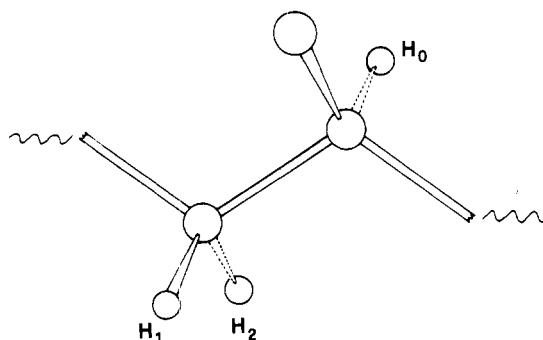


Figure 1.

Table I  
Comparison between Observed (at 150 °C for the Isotactic Polymer and 130 °C for the Syndiotactic Polymer) and Calculated (127 °C) Vicinal Proton Coupling Constants<sup>a</sup>

		obsd	calcd <sup>b</sup>			
			a	b	c	d
iso-tactic	$J_{01}$	7	7.5 (7.3)	6.7 (6.3)	4.7 (4.3)	4.9 (4.6)
	$J_{02}$	5.7	6.5 (7.6)	5.9 (6.6)	4.0 (4.5)	4.2 (4.8)
syndio-tactic	$J_{01}$	8.3	8.7 (7.7)	7.6 (6.7)	5.4 (4.7)	5.8 (5.1)
	$J_{02}$	4.8	6.0 (7.1)	5.2 (6.2)	3.4 (4.2)	3.6 (4.6)

<sup>a</sup> Calculated values are grouped according to the equation used. Numbers in parentheses refer to calculations performed with the energy maps reported in a previous paper.<sup>3</sup> For the numbering of  $J_{0k}$  ( $k = 1, 2$ ), see Figure 1. <sup>b</sup> (a)  $J = 7 - \langle \cos \varphi \rangle + 5 \langle \cos 2\varphi \rangle$ ; <sup>13a</sup> (b)  $J = 6.45 + 0.34 \langle \cos \varphi \rangle + 5.37 \langle \cos 2\varphi \rangle$ ; <sup>13b</sup> (c)  $J = 4.5 + 0.5 \langle \cos \varphi \rangle + 4.5 \langle \cos 2\varphi \rangle$ ; <sup>13a</sup> (d)  $J = A \langle \cos^2 \varphi \rangle + C$ . <sup>13c</sup>  $A = 8.5$  for  $0^\circ < \varphi < 90^\circ$  and  $A = 9.5$  for  $90^\circ < \varphi < 180^\circ$ ;  $C = -0.28$ .

the gauche–trans energy difference of *n*-butane.<sup>8</sup>

In practice, the second piece of information determines the size of the methyl group and the first, the size of the skeletal pseudoatoms.

As a byproduct of our analysis, we evaluated the probability maps of pairs of consecutive rotation angles, with or without imposing definite values to adjacent rotation angles. These maps will be discussed in the last section of the paper, with particular emphasis on the conformations required to invert a ...[G<sup>+</sup>T][G<sup>+</sup>T][G<sup>+</sup>T]... right-handed helical sequence into the left-handed sequence ...[TG<sup>-</sup>][TG<sup>-</sup>][TG<sup>-</sup>]... and vice versa<sup>9</sup> (the slashes indicate the methyl group placements; G<sup>+</sup>, T, and G<sup>-</sup> are skeletal rotation angles in the vicinity of 60, 180, and 300°).

The mathematical scheme used to obtain the chain partition function and the  $C_\infty$  characteristic ratio are the same as in ref 3, namely, the double-Fourier expansion of the correlation statistical weights and the pseudostereochemical equilibrium method. However, because of the difficulty involved in obtaining good percent accuracy for very low probability values while using the Fourier method, we have made recourse to straight matrix correlation products to obtain rotation angle probabilities, the individual matrices corresponding to a uniformly dense sampling of the energy surface.

### Conformational Energy Calculations

(a) **Geometrical Parameters.** These are reported in Table III and need no special comment insofar as they belong to the usual range. Following current approximations, they have been kept constant through the whole calculation process.

(b) **Nonbonded Interaction Parameters.** These are also reported in Table III. The Lennard-Jones 6/12 po-

Table II  
Experimental Values of Characteristic Ratios of Polypropylenes

	$C_\infty$	$T$ , °C	ref
isotactic	5.9	125	a
	5.6	143	a
	5.6	145	b
	5.0	183	c
	5.9	143	c
	6.4	125	c
	4.7	145	d
	5.8	145	e
atactic	5.5	129	a
	5.4	146	a
	5.4	153	b
	6.5	34	f
syndiotactic	6.7	45	g

<sup>a</sup> G. Moraglio, G. Gianotti, and U. Bonicelli, *Eur. Polym. J.*, **9**, 623 (1973). <sup>b</sup> J. B. Kinsinger and R. E. Hughes, *J. Phys. Chem.*, **67**, 1922 (1963). <sup>c</sup> A. Nakajima and A. Saijyo, *J. Polym. Sci., Part A-2*, **6**, 735 (1968). <sup>d</sup> F. Heatley, R. Salovey, and F. A. Bovey, *Macromolecules*, **2**, 619 (1969). <sup>e</sup> J. B. Kinsinger and R. E. Hughes, *J. Phys. Chem.*, **63**, 2002 (1959). <sup>f</sup> F. Danusso and G. Moraglio, *Makromol. Chem.*, **28**, 250 (1958). <sup>g</sup> H. Inagaki, T. Miyamoto, and S. Ohta, *J. Phys. Chem.*, **70**, 3420 (1966).

Table III  
Geometrical Parameters of the Polymer Chain and Parameters for Nonbonded Interactions:

$$V_{ij} = A_{ij}/r_{ij}^{12} - B_{ij}/r_{ij}^6{}^a$$

#### (1) Geometrical Parameters

	Bond Lengths, Å		
	C–C	C–H	
	1.54		1.09
	Bond Angles, Deg		
	C–C–C	Me <sup>b</sup> –C–C	
	112.0		112.0
	H–C <sup>T</sup> –C	H–C–H	108.0
	H–C <sup>S</sup> –C		109.2 <sup>c</sup>

#### (2) Nonbonded Interaction Parameters

	$10^{-3}A_{ij}$	$B_{ij}$	$r_{\min}$ , <sup>d</sup> Å
H...H	4.68	49	2.40
H...C	39.8	134	2.90
H...Me	121	367	2.95
C...C	294	381	3.40
C...Me	863	1024	3.45
Me...Me	2530	2750	3.50
Me'...Me' <sup>e</sup>	7550	2750	4.20

#### (3) Intrinsic Rotational Potential

$$V(\varphi) = 1.35(1 + \cos 3\varphi)$$

<sup>a</sup>  $r_{ij}$  in Å;  $V_{ij}$  in kcal/mol (1 kcal = 4.184 kJ). <sup>b</sup> Symbol Me indicates the methyl group pendant to the chain. <sup>c</sup> C<sup>T</sup> and C<sup>S</sup> indicate, respectively, a tertiary and a secondary carbon atom. <sup>d</sup> The distances refer to the minimum of the nonbonded interaction energy functions. <sup>e</sup> Symbol Me' indicates a pseudoatom which takes into account the mean steric effect between the remaining chain atoms before and after the chain segment under investigation (see text for more details).

tential has been adopted throughout. As for the atom pairs involving C and H only, the parameters are essentially identical with those already used by us for polypropylene within the Lennard-Jones approximation.<sup>2,3</sup>

The methyl group has been treated in a way analogous to that used in our previous work (Me in Table III).<sup>2,3</sup> We emphasize that the  $B$  parameters for the CH<sub>3</sub>...X interactions were derived following the Slater–Kirkwood approximation,<sup>10</sup> attributing an effective electron number of 22 to the methyl group;<sup>11</sup> the corresponding  $A$  parameters were calculated by imposing that each pairwise energy

function has its own minimum at the sum of the two van der Waals radii. As anticipated, the methyl radius ( $r_{\text{Me}} = 1.75 \text{ \AA}$ ) was chosen as to fit the observed gauche-trans energy difference for *n*-butane (observed  $\sim 0.8 \text{ kcal/mol}$ ,<sup>8</sup> calculated  $0.74 \text{ kcal/mol}$ ; between the minimal rotation angles  $\varphi_{\text{G}} = 70^\circ$ ,  $\varphi_{\text{T}} = 180^\circ$ , and  $\text{C-C-C} = 112^\circ$ ). Consequently, the values previously used by us<sup>3</sup> were somewhat too large; e.g., with  $r_{\text{Me}} = 1.85 \text{ \AA}$  the above energy difference becomes about  $1.5 \text{ kcal/mol}$ . Admittedly, the bond angle flexibility may substantially lower this figure; nevertheless, the present choice of the methyl radius appears to be self-consistent insofar as we explicitly neglect any such flexibility effect in the present work.

According to the foregoing discussion, the skeletal atoms were considered as normal C atoms except when the interactions between two of them separated by four bonds were computed, in which case they were treated as pseudoatoms ( $\text{Me}'$  in Table III) larger than the methyl groups, although, for simplicity, with the same attractive parameter. These special interactions are meant to approximately take into account the mean steric effect involving atoms separated by more than four bonds, inevitably missed in our statistical description. That such long-range interactions may be important indeed will be shown in the following.

Let  $\varphi_1\varphi_2\varphi_3\varphi_4$  be any four consecutive rotation angles on the carbon skeleton and  $E(\varphi_1\varphi_2\varphi_3\varphi_4)$  the conformational energy of the chain section, the geometry of which is fully defined by the four angles. Obviously enough, this energy will be given by the sum of the four intrinsic rotational contributions (see Table III, section 3) plus the nonbonded terms. If, according to current approximations, the energy of any conformation may be split into contributions depending on two angles each, we may write

$$E(\varphi_1\varphi_2\varphi_3\varphi_4) = E(\varphi_1\varphi_2) + E(\varphi_2\varphi_3) + E(\varphi_3\varphi_4) \quad (1)$$

where  $E(\varphi_i\varphi_{i+1})$  may be calculated with different nonbonded interaction parameters in order to produce a better fit in the above (approximate) equality. (Besides, the three  $E(\varphi_i\varphi_{i+1})$  functions must be evaluated in such a way that no energy term is accounted for more than once.) Suppose now that there are appreciable differences between the two sides of eq 1 because of the nonbonded interactions depending on more than two consecutive  $\varphi$ 's. How can we obtain an average measure of these contributions for fixed  $\varphi_2$  and  $\varphi_3$ ? It seems reasonable to take the effective energy of the ensemble of the conformations with fixed  $\varphi_2$  and  $\varphi_3$  as the free energy evaluated over the remaining variables (i.e., in our case  $\varphi_1$  and  $\varphi_4$ ). Consequently, we will identify the best average measure of the longer range interactions with the difference between the free energies of either side of eq 1, calculated over all possible values of  $\varphi_1$  and  $\varphi_4$ . We have, therefore

$$\Delta E(\varphi_2\varphi_3) = A(\langle \varphi_1 \rangle \varphi_2 \varphi_3 \langle \varphi_4 \rangle) - A(\langle \varphi_1 \rangle \varphi_2) - A(\varphi_3 \langle \varphi_4 \rangle) - E(\varphi_2\varphi_3) \quad (2)$$

where the  $A$  terms are given by eq 3.

$$A(\langle \varphi_1 \rangle \varphi_2 \varphi_3 \langle \varphi_4 \rangle) = -RT \ln \left[ \int_{\varphi_1} \int_{\varphi_4} \exp(-E(\varphi_1\varphi_2\varphi_3\varphi_4)/RT) d\varphi_1 d\varphi_4 \right] \quad (3a)$$

$$A(\langle \varphi_1 \rangle \varphi_2) = -RT \ln \left[ \int_{\varphi_1} \exp(-E(\varphi_1\varphi_2)/RT) d\varphi_1 \right] \quad (3b)$$

$$A(\varphi_3 \langle \varphi_4 \rangle) = -RT \ln \left[ \int_{\varphi_4} \exp(-E(\varphi_3\varphi_4)/RT) d\varphi_4 \right] \quad (3c)$$

We have limited our consideration to three rotational pairs, namely (see Figure 2), (1)  $\varphi_2 = \varphi_{2i} = 280^\circ$ ,  $\varphi_3 = \varphi_{2i+1} = 80^\circ$ , (2)  $\varphi_2 = \varphi_{2i-1} = 80^\circ$ ,  $\varphi_3 = \varphi_{2i} = 280^\circ$ , and (3)  $\varphi_2 =$

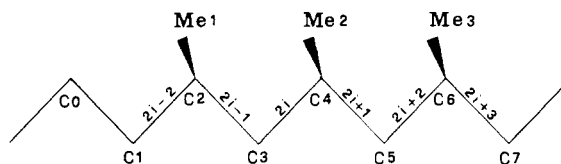


Figure 2.

$\varphi_{2i-1} = 60^\circ$ ,  $\varphi_3 = \varphi_{2i} = 190^\circ$ . These conformations correspond to relative minima of the potential energy in ref 2 and 3. The potential energy functions  $E(\varphi_i\varphi_{i+1})$  were evaluated according to previously followed criteria,<sup>2,3</sup> i.e., identifying with  $\text{Me} \cdots \text{Me}$  the interactions between skeletal C atoms separated by four bonds ( $r_{\text{Me}} = 1.75 \text{ \AA}$ ). This was not the case for  $E(\varphi_1\varphi_2\varphi_3\varphi_4)$ , where all the skeletal atoms were treated as carbons except for the pair separated by six bonds, in which case a  $\text{Me} \cdots \text{Me}$  interaction was assumed. The values of  $\Delta E(\varphi_2\varphi_3)$  were 6.2, 2.0, and 0.1 kcal/mol for the pairs (1), (2), and (3) above. The relatively large figures obtained in the first two cases clearly demonstrate the significant role of the interactions between atoms more than four bonds apart. Incidentally, Suter and Flory already recognized the existence of this effect, at least in the vicinity of the first conformation discussed above (see their forbidding the  $g(g^*)/g(g^*)$  sequences in the  $\mathbf{U}'$  matrix).<sup>6</sup> Identification of the terminal atoms of the four-bond skeletal sequences with methyl groups is obviously insufficient to account for the longer range interactions. It must be pointed out that in the first two cases, unlike the third one, the skeletal atoms four bonds apart approach their closest acceptable distance ( $\sim 3.2 \text{ \AA}$ ). Consequently, it seems a natural suggestion that an appropriate potential between them may approximately account for the average steric effect between their pendant atoms. It might be argued that similar, ad hoc potentials should be adopted for any pairwise interaction involving the skeletal atoms; it is possible to see that this is not the case. Let us first consider the three-bond interactions.

With reference to Figure 2, the interaction between any substituent of  $\text{C}_2$  with  $\text{Me}_2$ , e.g., is fully specified by the two consecutive rotation angles  $\varphi_{2i-1}$  and  $\varphi_{2i}$ , and therefore it need not be incorporated into  $\text{C}_2$ . It could be objected that the four-bond interactions such as  $\text{C}_1 \cdots \text{Me}_2$  should be treated by allowing some special bulkiness to  $\text{C}_1$  to account for the  $\text{C}_0 \cdots \text{Me}_2$  interaction, contrary to what is done with our scheme. However this last interaction is already implicit into the  $\text{C}_0 \cdots \text{C}_4$  nonbonded energy, which is calculated as between bulky atoms.

In conclusion, the skeletal four-bond interactions (indicated as  $\text{Me}' \cdots \text{Me}'$ ) (Table III, section 2) show that, although their attractive parameter  $B$  is the same as between methyl groups, the repulsive parameter  $A$  is larger. Its value was chosen with the empirical criterion of a good fit with the experimental data, under the requirement that the van der Waals radius of the  $\text{Me}'$  pseudoatoms should not depart very much from  $2 \text{ \AA}$  (it turns out that  $r_{\text{Me}'} = 2.10 \text{ \AA}$ , since  $r_{\text{min}}(\text{Me}' \cdots \text{Me}') = 2r_{\text{Me}'} = 4.20 \text{ \AA}$ ; cf. Table III). For reasons of simplicity, and in view of the model approximations, no difference was assumed between the tertiary-tertiary ( $\text{C}_2 \cdots \text{C}_6$  in Figure 2) and the secondary-secondary ( $\text{C}_1 \cdots \text{C}_5$ ) interactions.

(c) **Energy Maps.** The three independent energy maps, each of which depends on two consecutive skeletal rotations, are reported in Figure 3. With reference to Figure 2,  $E_{dd}$  (Figure 3a) and  $E_{dl}$  (Figure 3b) depend on the rotation angles  $\varphi_{2i-1}$  and  $\varphi_{2i}$  ( $d$  and  $l$  refer to the configurations of the adjacent tertiary C atoms of the chain). As an example, in Figure 2 *d* configurations are shown only. The  $E_d$  map (Figure 3c) depends on  $\varphi_{2i}$  and  $\varphi_{2i+1}$ , the

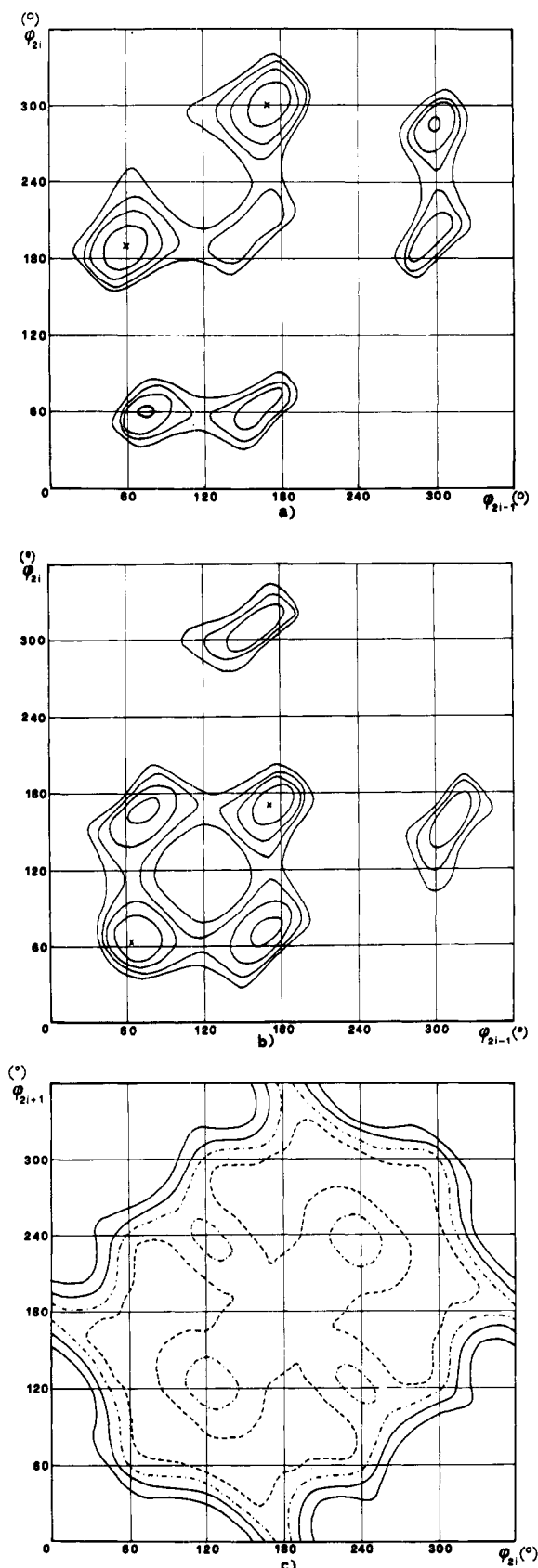


**Figure 3.** Internal conformational energy plots  $E_{dd}$  (a),  $E_{dl}$  (b), and  $E_d$  (c). The symbols  $d$  and  $l$  refer to whether the methyl groups point above or below in Figure 2. The first two maps depend on pairs of consecutive skeletal rotations (in degrees) comprised between two tertiary C atoms and the third map on pairs of consecutive rotations astride a tertiary atom. In maps a and b, energy levels are drawn at 4 (outer curve), 3, 2, and 1 kcal/mol above the minima ( $\times$ ), while in c, they are at 2 (outer curve), 1, 0.5 (---), and 0.1 (---) kcal/mol.

tertiary C atom being in the  $d$  configuration.  $E_l$ ,  $E_{ll}$ , and  $E_{ld}$  can be obtained by  $E_d$ ,  $E_{dd}$ , and  $E_{dl}$ , respectively, by merely reversing the signs of the corresponding  $\varphi$ 's.  $E_{dd}$  and  $E_{dl}$  were calculated by adding together the nonbonded interaction terms depending on either  $\varphi_{2i-1}$  or  $\varphi_{2i}$  or both, as well as the intrinsic rotational potentials depending on both  $\varphi_{2i-1}$  and  $\varphi_{2i}$  (see Table III, section 3). To avoid overcounting energy contributions,  $E_d$  was only obtained from the nonbonded interactions depending on both  $\varphi_{2i}$  and  $\varphi_{2i+1}$ ; since these do not involve side methyl groups (see Figure 2), the resulting map is highly symmetrical insofar as  $E_d(\varphi_A\varphi_B) = E_d(\varphi_B\varphi_A)$  and also  $E_d(\varphi_A\varphi_B) = E_d(-\varphi_B-\varphi_A)$ . ( $\varphi_A$  and  $\varphi_B$  are specific values attributed to  $\varphi_{2i-1}$  and  $\varphi_{2i}$ .) As a consequence we have  $E_d(\varphi_A\varphi_B) = E_l(\varphi_A\varphi_B)$ . The  $E_{dd}$  and  $E_{dl}$  maps display a lower symmetry, namely,  $E_{dd}(\varphi_A\varphi_B) = E_{dd}(-\varphi_B\varphi_A)$ , while  $E_{dl}(\varphi_A\varphi_B) = E_{dl}(\varphi_B\varphi_A)$ .

All the energy values were evaluated at intervals of  $10^\circ$  along both angles. The resulting  $36 \times 36$  grids of weighted points were then interpolated to produce the energy maps reported in Figure 3.

**(d) Probability of Rotational Sequences.** The general approach to this problem is illustrated in ref 7, pp 75-80; each point on the  $36 \times 36$  grid representing the general  $E$  map was formally considered as the equivalent of a rotational isomeric state. We report here the basic equations used by us in treating the specific cases of iso- and syndiotactic polypropylenes.

Each potential energy grid was converted into the corresponding statistical weight matrix  $U$  by substituting  $E$  with  $w = \exp(-E/RT)$ .

Let us first consider the isotactic case. As a definition

$$U = U_d \cdot U_{dd} \quad (4)$$

where  $U_d$  and  $U_{dd}$  obviously correspond to  $E_d$  and  $E_{dd}$ .<sup>3</sup> In the following we will introduce the simplifying notation that any matrix element will be denoted by the pair of its corresponding angles. As an example,  $U(\varphi_A\varphi_B)$  refers to the element of  $U$  whose row and column, respectively, correspond to the rotations  $\varphi_A$  and  $\varphi_B$ . The probability of a given rotation on any even and odd bond (see Figure 2) is given by

$$p_{\text{even}}(\varphi) = \mathbf{a}^*(\varphi) \cdot \mathbf{a}(\varphi) \quad (p_{\text{odd}}(\varphi) = p_{\text{even}}(-\varphi)) \quad (5)$$

where  $\mathbf{a}^*(\varphi)$  and  $\mathbf{a}(\varphi)$ , respectively, are the elements corresponding to the angle  $\varphi$  in the row and column eigenvectors of the largest eigenvalue  $\lambda$  of  $U$ . In order to get accurate values of  $\lambda$ ,  $\mathbf{a}^*$  and  $\mathbf{a}$ , we used the iterative self-multiplication of  $U$ , exploiting the relationship

$$\lim_{n \rightarrow \infty} U^n = \lambda^n \cdot \mathbf{a}^T \cdot \mathbf{a}^* \quad (6)$$

$$\mathbf{a}^T = \text{transpose of } \mathbf{a}$$

In Figure 4a the probability plot of  $p_{\text{odd}}(\varphi)$  vs.  $\varphi_{2i-1}$  is reported.

As for the syndiotactic polymer, it is convenient to adopt the following matrix arrangement. If the increasing order of values (i.e.,  $\varphi = 0, 10, 20^\circ, \dots$ ) is the normal one, let the decreasing order (i.e.,  $\varphi = 0, -10, 20^\circ, \dots$ ) be adopted for the second rotation angle appearing in  $U_{dl}$  and for the first one in  $U_{ld}$ ; this formally produces  $U_{dl} = U_{ld}$ , while keeping  $U_d = U_l$ . The  $U$  matrix in this case may be conveniently expressed as

$$U = U_d \cdot U_{dl} \quad (7)$$

and the above results still formally apply. Henceforth, the iso- and syndiotactic polymers will be treated under the same formalism. The above technical solution is analogous to that used by Flory in ref 7, p 223.

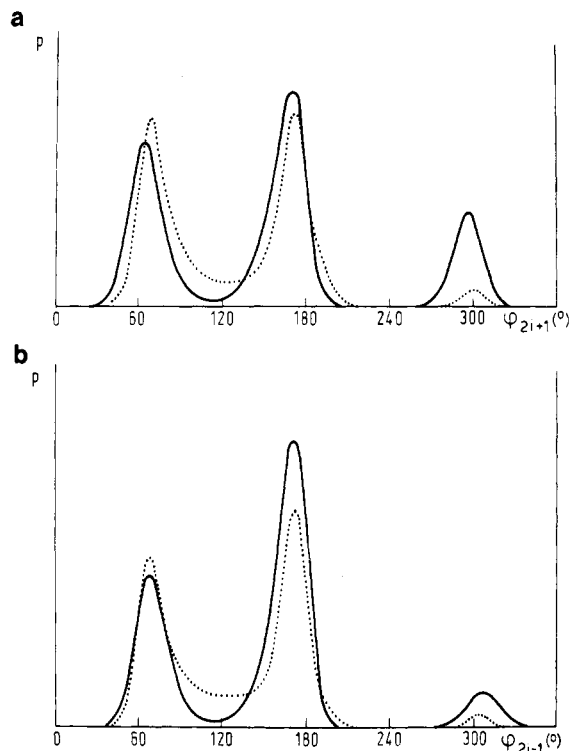


**Figure 4.** Probability plots  $p_{\text{odd}}$  vs.  $\varphi_{2i-1}$  (see Figure 2 and eq 5) for isotactic (above) and syndiotactic (below) polypropylenes calculated at 400 K. Dotted curves refer to earlier energy maps.<sup>3</sup> The scale of  $p$  is arbitrary although consistent throughout. Angles are in degrees.

The probability of any sequence of two rotation angles  $p_d(\varphi_{2i}\varphi_{2i+1})$ <sup>12</sup> (see Figure 2) is given by

$$p_d(\varphi_{2i}\varphi_{2i+1}) = \mathbf{a}^* \cdot \mathbf{U}_d'(\varphi_{2i}\varphi_{2i+1}) \cdot \mathbf{U}_{dx} \cdot \mathbf{a}^T / \lambda \quad (8)$$

where  $\mathbf{U}_d'(\varphi_{2i}\varphi_{2i+1})$  is obtained by  $\mathbf{U}_d$  after striking off all elements except the one which corresponds to the intersection of  $\varphi_{2i}$  and  $\varphi_{2i+1}$ .  $\mathbf{U}_{dx}$  stands for either  $\mathbf{U}_{dd}$  or  $\mathbf{U}_{dl}$ , depending on which polymer is considered. If the bond pair is  $\varphi_{2i-1}\varphi_{2i}$  the probability is

$$p_{dx}(\varphi_{2i-1}\varphi_{2i}) = \mathbf{a}^* \cdot \mathbf{U}_d''(\varphi_{2i-1}\varphi_{2i}) \cdot \mathbf{a}^T / \lambda \quad (9)$$

where the meaning of the symbols is evident.

Suppose  $\varphi_{2i-2}$  and  $\varphi_{2i+3}$  (see Figure 2) have fixed values. In that case it is possible to prove that the conditional probability  $\bar{p}_d(\varphi_{2i}\varphi_{2i+1})$  is given by

$$\bar{p}_d(\varphi_{2i}\varphi_{2i+1}) = \mathbf{a}^* \cdot (\mathbf{U}_d''(\varphi_{2i-2}) \cdot \mathbf{U}_{dx} / \lambda) \cdot (\mathbf{U}_d'(\varphi_{2i}\varphi_{2i+1}) \cdot \mathbf{U}_{dx} / \lambda) \cdot (\mathbf{U}_d'''(\varphi_{2i+3}) \cdot \mathbf{U}_{dx} / \lambda) \cdot \mathbf{a}^T \quad (10)$$

where  $\mathbf{U}_d''(\varphi_{2i-2})$  and  $\mathbf{U}_d'''(\varphi_{2i+3})$ , respectively, derive from  $\mathbf{U}_d$  after striking off all the rows except that of  $\varphi_{2i-2}$  and all the columns except that of  $\varphi_{2i+3}$ .

For the sake of comparison with the energy plots, we have thought it useful to present the bidimensional probability results under the free-energy form, e.g.

$$A(\varphi_A\varphi_B) = -RT \ln p(\varphi_A\varphi_B) \quad (11)$$

Unless otherwise stated, all the results have been obtained at  $T = 400$  K ( $=127^\circ\text{C}$ ).

### Discussion of the Results

Figure 4 shows the plots of the probability vs. the rotation angle  $\varphi_{2i-1}$  (see Figure 2) for iso- and syndiotactic polypropylenes, according to eq 5. The analogous plots derived from our earlier energy maps<sup>3</sup> are also reported at the same temperature (i.e.,  $T = 400$  K). The coupling constants  $J_{01}$  and  $J_{02}$  (see Figure 1) have been computed by adopting four different current versions of the Karplus

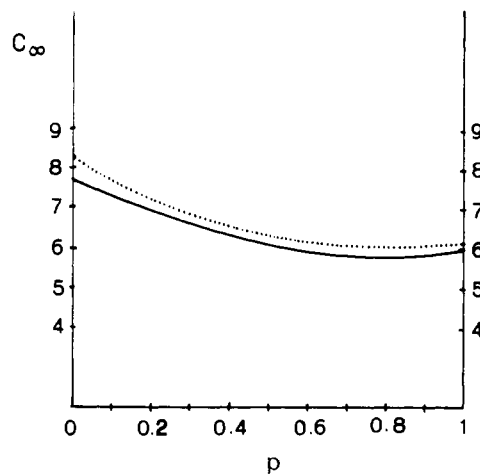


**Figure 5.** Plots of  $C_\infty$  vs.  $p$  (probability of a meso dyad, i.e., of an isotactic placement). The solid line is calculated at 400 K and the dotted line at 375 K.

equation<sup>13</sup> which relate  $J_{0k}$  with the statistical distribution of the rotation angles  $\varphi_{0k}$  characterizing the sequence  $\text{H}_0\text{--C--C--H}_k$  ( $\varphi_{0k}$  is very simply related with the corresponding angle that refers to the skeletal sequence). The equations are reported in Table I, and the obvious connection of any cosine average with the rotation probabilities is  $\langle \cos(n\varphi) \rangle = \int_0^{2\pi} \cos(n\varphi) p(\varphi) d\varphi$ . The results are given in Table I both for the present and for the earlier energy results.<sup>3</sup> It is apparent that the new values are in much better agreement with experiment; we will specifically refer, in the following, to equation b which appears to fit best among the four. (It is worth mentioning that the parameters appearing therein were obtained by Ferro et al.<sup>13b</sup> by a least-squares fit to the coupling constants of different stereoisomers of 1,3,5,7-tetramethylcyclooctane.) Obviously enough, we do not claim that only our approach may produce good results in this respect; in fact, the earlier conformational results by Suter and Flory<sup>6</sup> also appear to produce good agreement with the experimental  $J$ 's when the same equations are used.<sup>14</sup> On the other hand, we want to stress that these authors have also taken care of the interactions between distant atoms, at least to some extent, by forbidding few appropriate rotational pairs in their  $\mathbf{U}'$  matrix.<sup>6</sup>

The characteristic ratio  $C_\infty$  calculated for polypropylene chains with different statistical distributions of  $d$  and  $l$  stereoisomeric centers is reported in Figure 5. The pseudostereochemical equilibrium approach was followed as in ref 3;  $p$  is the Markoffian probability of a  $dd$  dyad, so that  $p = 0$  and  $1$  correspond to perfectly syndio- and isotactic chains, respectively, while  $p = 0.5$  stands for a completely random atactic polymer. The results are reported for  $T = 375$  K (dotted line) and  $400$  K (solid line) and must be compared with the experimental values obtained from  $\Theta$  solutions given in Table II. Considering the experimental uncertainties as well as the model approximations, the agreement is rather good. Unlike our previous results,<sup>3</sup> the minimum at intermediate  $p$  values is virtually nonexistent, thus producing better consistency with the experimental data known so far. The most serious disagreement is related with the syndiotactic polymer for which the calculated value (8.3 at  $102^\circ\text{C}$ ) is larger than the single experimental datum available (6.7 at  $45^\circ\text{C}$ ). The discrepancy may be substantially smaller if one considers that all the syndiotactic polypropylene samples prepared so far contain a substantial ( $\sim 5\%$ ) amount of steric defects.<sup>15,6</sup> As for the temperature coefficient  $d \ln \langle r^2 \rangle_0 / dT$ , we obtain, from the plots given in Figure 5,  $-2.7$

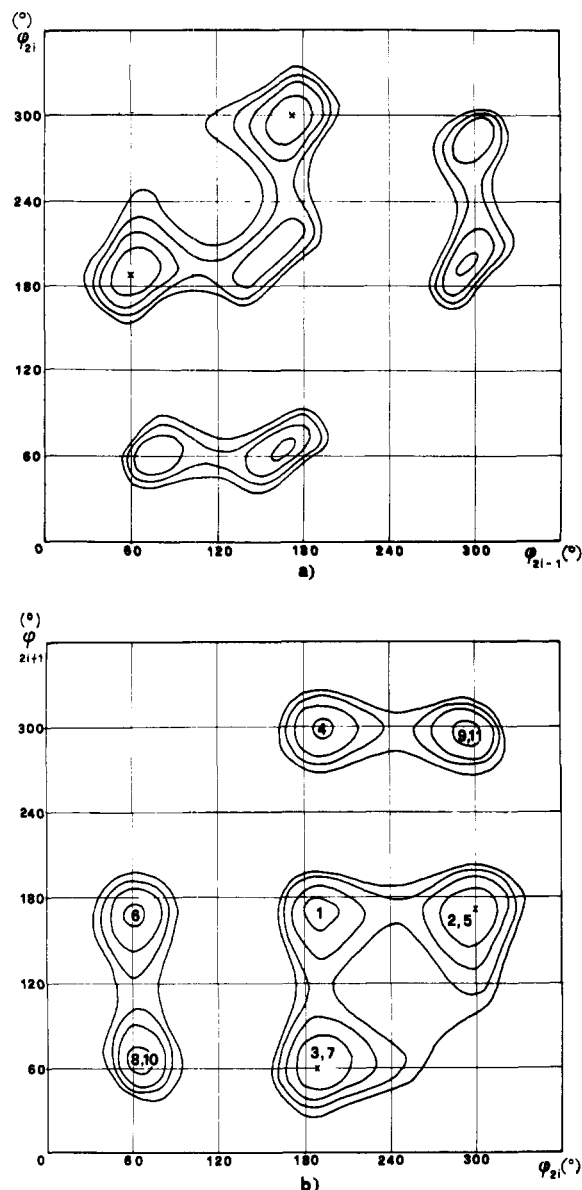


**Figure 6.** Isotactic polypropylene: plots of the free energy  $A_{dd}(\varphi_{2i-1}\varphi_{2i})$  (a) and  $A_{dd}(\varphi_{2i}\varphi_{2i+1})$  (b) for pairs of consecutive skeletal rotations (see eq 11). Contours are drawn as in Figure 3a,b.  $A_d$  is very similar to the corresponding conditional free energy for fixed values of  $\varphi_{2i-2} = 190^\circ (\approx T)$  and of  $\varphi_{2i+3} = 170^\circ (\approx T)$ ; consequently, numbers from 1 to 10 indicate the relative conformational minima fully detailed in Table IVB.

$\times 10^{-3}$  and  $-0.9 \times 10^{-3}$ , respectively, for the syndio- and isotactic polymers, with smoothly changing values for intermediate  $p$ 's. On the whole, these figures are in better agreement with experiment (cf. Table VIII of ref 6) than the older ones,<sup>3</sup> especially because the absolute figure for the isotactic polymer ( $3.6 \times 10^{-3}$ ) was much larger than the experimental value ( $\leq 1.5 \times 10^{-3}$ ).<sup>6</sup>

Figure 6 shows the local free-energy plots  $A_{dd}(\varphi_{2i-1}\varphi_{2i})$  and  $A_{dd}(\varphi_{2i}\varphi_{2i+1})$  (see Figure 2 for the labeling of rotation angles) calculated for the isotactic polymer through eq 8, 9, and 11. The first map (Figure 6a) is similar to the corresponding internal energy map  $E_{dd}$  (see Figure 3a), while the second one is markedly different from its corresponding  $E_d$  map (Figure 3c) because, unlike  $E_{dd}$ ,  $E_d$  only contains the nonbonded interaction terms depending on both  $\varphi_{2i}$  and  $\varphi_{2i+1}$ . In spite of the similarity, it is worth pointing out that  $A_{dd}$  differs from  $E_{dd}$  insofar as the minima involving rotation angles close to trans have a relatively lower value in  $A_{dd}$  than in  $E_{dd}$ . More precisely,

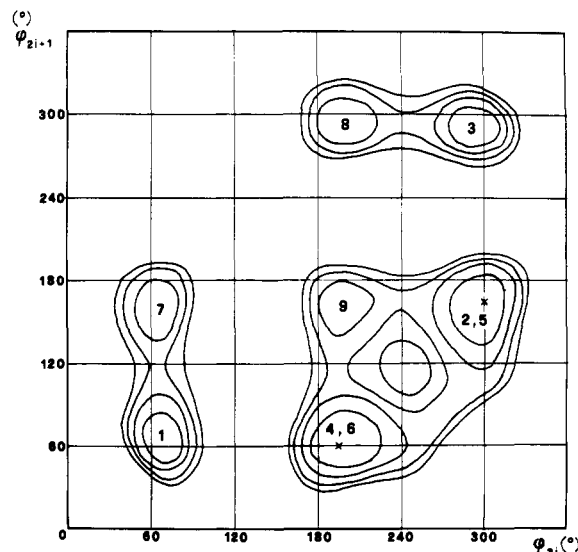


**Figure 7.** Isotactic polypropylene: plot of the conditional free energy  $\bar{A}'_d(\varphi_{2i}\varphi_{2i+1})$  for fixed values of  $\varphi_{2i-2} = 300^\circ (\equiv G^-)$  and of  $\varphi_{2i+3} = 60^\circ (\equiv G^+)$ . Contours are drawn as in Figure 3a,b. Numbers from 1 to 9 indicate the relative conformational minima fully detailed in Table IVA.

replacing a G with a T state in  $A_{dd}$  implies an average energy decrease that is about 1.5 kcal/mol larger than the corresponding amount in  $E_{dd}$ . Since the free energy is directly related to probability (see eq 8), this conclusion implies that the trans states are more probable than predicted on the basis of the local internal energy alone. It is possible to show that this is typical rotation-correlation effect, since a T state may be followed by either T or G with less severe restrictions than a G state (e.g., the  $G^+G^+$  pairs are always forbidden). (Although the whole spectrum of the rotation angles was used in our calculations throughout, we will henceforth refer, for practical reasons, to the rotational minima of the potential energy in terms of  $G^+$ , T, and  $G^-$ , where deviations of up to  $25^\circ$  from the ideal values of  $60^\circ$ ,  $180^\circ$ , and  $300^\circ$  may occasionally occur.) It is worth pointing out from Figure 6a,b that the usual description of the isotactic polypropylene chain in terms of  $\dots[G^+T][G^+T]\dots$  and  $\dots[TG^-][TG^-]\dots$  equivalent helical sequences may still be maintained for convenience, in view of their relatively high probability, as it may be checked on the free-energy maps. Consequently, we have thought it useful to investigate in some detail the still open problem of the conformational inversions between the two sequences.<sup>9,16</sup>

At first, we directed our attention to the conditional free-energy maps  $\bar{A}_d(\varphi_{2i}\varphi_{2i+1})$ , obtained by giving definite values to both  $\varphi_{2i-2}$  and  $\varphi_{2i+3}$  (see Figure 2 and eq 10 and 11). In particular, let us denote as  $\bar{A}'_d$  the map with  $\varphi_{2i-2} = 300^\circ (\equiv G^-)$  and  $\varphi_{2i+3} = 60^\circ (\equiv G^+)$ , and as  $\bar{A}''_d$  the map with  $\varphi_{2i-2} = 190^\circ (\approx T)$  and  $\varphi_{2i+3} = 170^\circ (\approx T)$ . It is easy to see that  $\bar{A}'_d$  (Figure 7) maps the local conformations leading from the helical  $\dots[TG^-][TG^-]\dots$  sequence (sequence  $\alpha$ ) to its opposite  $\dots[G^+T][G^+T]\dots$  (sequence  $\beta$ );<sup>9</sup> these "inversion" conformations are assumed to be confined within two monomer units, i.e.,  $\dots G^-|\varphi_{2i-1}\varphi_{2i}|\varphi_{2i+1}\varphi_{2i+2}|G^+\dots$ . It is important to realize that the only variables appearing in Figure 7 are  $\varphi_{2i}$  and  $\varphi_{2i+1}$ , while  $\varphi_{2i-1}$  and  $\varphi_{2i+2}$  are allowed to vary in all possible ways. As for  $\bar{A}''_d$ , it analogously maps the  $\dots T|\varphi_{2i-1}\varphi_{2i}|\varphi_{2i+1}\varphi_{2i+2}|T\dots$  conformations, corresponding to the alternative inversions from sequence  $\beta$  to  $\alpha$ . From comparison of Figure 7 with Figure 6b, it is an obvious conclusion that it is more difficult to have a T state on either  $\varphi_{2i}$  or  $\varphi_{2i+1}$  by assigning gauche states to both  $\varphi_{2i-2}$

Table IV  
Most Probable Conformations for Helix Inversion  
in Isotactic Polypropylene<sup>a</sup>

(A) Inversion from ... TG <sup>+</sup> TG <sup>+</sup> ... to ... G <sup>+</sup> T G <sup>+</sup> T ...		
conformation (...G <sup>+</sup>   $\varphi_{2i-1}\varphi_{2i}$   $\varphi_{2i+1}\varphi_{2i+2}$  G <sup>+</sup> ...)	energy, kcal/mol	index no. of the min <sup>b</sup>
...G <sup>+</sup>  TG <sup>+</sup>  G <sup>+</sup> T G <sup>+</sup> ...	$\Delta$	1
...G <sup>+</sup>  TG <sup>+</sup>  TG <sup>+</sup>  G <sup>+</sup> ...	$\Delta$	2
...G <sup>+</sup>  TG <sup>+</sup>  G <sup>+</sup> T G <sup>+</sup> ...	$\Delta$	3
...G <sup>+</sup>  G <sup>+</sup> T G <sup>+</sup> T G <sup>+</sup> ...	$\Delta$	4
...G <sup>+</sup>  TG <sup>+</sup>  TT G <sup>+</sup> ...	$\Delta + 0.6$	5
...G <sup>+</sup>  TT G <sup>+</sup> T G <sup>+</sup> ...	$\Delta + 0.6$	6
...G <sup>+</sup>  TG <sup>+</sup>  TG <sup>+</sup>  G <sup>+</sup> ...	$\Delta + 1.4$	7
...G <sup>+</sup>  G <sup>+</sup> T G <sup>+</sup> T G <sup>+</sup> ...	$\Delta + 1.4$	8
...G <sup>+</sup>  G <sup>+</sup> T TG <sup>+</sup>  G <sup>+</sup> ...	$\Delta + 1.8$	9
(B) Inversion from ... G <sup>+</sup> T G <sup>+</sup> T ... to ... TG <sup>+</sup> TG <sup>+</sup> ...		
conformation (...T  $\varphi_{2i-1}\varphi_{2i}$   $\varphi_{2i+1}\varphi_{2i+2}$  T...)	energy, kcal/mol	index no. of the min <sup>c</sup>
...T G <sup>+</sup> T TG <sup>+</sup>  T...	$\Delta'$	1
...T TG <sup>+</sup>  TG <sup>+</sup>  T...	$\Delta'$	2
...T G <sup>+</sup> T G <sup>+</sup> T T...	$\Delta'$	3
...T G <sup>+</sup> T G <sup>+</sup> G <sup>+</sup>  T...	$\Delta' + 0.6$	4
...T G <sup>+</sup> G <sup>+</sup>  TG <sup>+</sup>  T...	$\Delta' + 0.6$	5
...T G <sup>+</sup> G <sup>+</sup>  TG <sup>+</sup>  T...	$\Delta' + 0.6$	6
...T G <sup>+</sup> T G <sup>+</sup> G <sup>+</sup>  T...	$\Delta' + 0.6$	7
...T G <sup>+</sup> G <sup>+</sup>  G <sup>+</sup> T T...	$\Delta' + 1.0$	8
...T TG <sup>+</sup>  G <sup>+</sup> G <sup>+</sup>  T...	$\Delta' + 1.0$	9
...T TG <sup>+</sup>  G <sup>+</sup> T T...	$\Delta' + 1.6$	10
...T TG <sup>+</sup>  G <sup>+</sup> T T...	$\Delta' + 1.6$	11

<sup>a</sup> The energy parameters  $\Delta$  and  $\Delta'$  are 0.9 and 0.7 kcal/mol, respectively. <sup>b</sup> See Figure 7. <sup>c</sup> See Figure 6b.

and  $\varphi_{2i+3}$  than after removing this restriction. The minima shown in Figure 7 are detailed in Table IVA; the values of  $\varphi_{2i-1}$  and  $\varphi_{2i+2}$  were derived from analysis of the most important terms of the partition function contributing to the free energy reported in Figure 7. The alternative conditional free-energy map  $\bar{A}_d'$  is quite analogous to  $E_d$  (see Figure 6b); therefore it is not explicitly reported. As done with Figure 7 and Table IVA for the ...G<sup>+</sup>...|...|G<sup>+</sup>... inversions, the minima of Figure 6b are also detailed in Table IVB in terms of the ...T|...|...|T... inversions. The parameters  $\Delta$  and  $\Delta'$  appearing in Table IV correspond to the lowest energy values for the inversion of either type (i.e., 0.9 and 0.7 kcal/mol, respectively). Remembering that in a very long chain each inversion of type  $\alpha/\beta$  is always followed by an inversion of type  $\beta/\alpha$ , the most significant conclusions to be drawn from Table IV are as follows:

(i) The minimum energy value required to perform an inversion pair is 1.6 kcal/mol (i.e.,  $\Delta + \Delta'$ ).

(ii) Unlike previous conclusions by one of the authors,<sup>9</sup> it appears that the easiest inversion sequence  $\alpha/\beta$  (see Table IVA) happens via a ...|TG<sup>+</sup>|G<sup>+</sup>T|... conformation, while the modified ...|TG<sup>+</sup>|G<sup>+</sup>T|... conformations<sup>9</sup> seem to be essentially forbidden.

(iii) It is confirmed that the easiest inversion of the alternative type (i.e., sequence  $\beta/\alpha$ ; see Table IVB) happens via a ...|G<sup>+</sup>T|TG<sup>+</sup>|... conformation.

We will not report here the conformational analysis of the syndiotactic polymer with the same detail as for the isotactic case. However, the basic conclusions may be summarized as follows:

(i) It is confirmed that the lowest energy local conformations are |TT| and |GG| and that |GG| cannot follow to

itself while |TT| suffers no constraints.

(ii) Unlike previous conclusions,<sup>9</sup> introduction of a |GG| between two |TT| pairs appears to decrease the energy by 0.4 kcal/mol, which may be the reason for the higher stability of the twofold helix ...|TT|GG|TT|GG|...<sup>17</sup> compared with the planar zigzag ...|TT|TT|... in the crystalline state.<sup>18</sup> This stabilization effect is fully related with the van der Waals attraction between the "bulky" skeletal atoms separated by four bonds when they are close to their lowest energy distance.

(iii) At the expense of 0.5 kcal/mol, the |TG<sup>+</sup>| or |G<sup>+</sup>T| pairs (for a *dl* dyad) may also be affected, while no ...G|G... pair may exist in any case.

## Concluding Remarks

It is worth pointing out that, in spite of its apparent complexity, the present approach, based on the entire analysis of the configurational space of skeletal rotations, provides a simple, automatic-working device to obtain the statistical averages of polymer chains. In particular, there is no need either to define the local energy minima or to evaluate their partition functions separately. Admittedly, the uncertainties related with the choice of the nonbonded interaction parameters as well as with the interactions between relatively distant atoms (five to seven bonds apart) still leave an appreciable margin of possible error. As for the distant-atom interactions, we have proposed an empirical although, we believe, reasonable way out. Perhaps, a systematic application of our method of evaluating average values of these interactions might be worthwhile.

**Acknowledgment.** We gratefully acknowledge useful information repeatedly received by Dr. Tonelli. This work was supported by a contribution (No. 77.00628.03) from the Consiglio Nazionale delle Ricerche.

## References and Notes

- (1) A. Zambelli, M. G. Giongo, and G. Natta, *Makromol. Chem.*, **112**, 183 (1968).
- (2) G. Allegra, M. Calligaris, L. Randaccio, and G. Moraglio, *Macromolecules*, **6**, 397 (1973).
- (3) G. Allegra and S. Brückner, *Macromolecules*, **10**, 106 (1977).
- (4) R. H. Boyd and S. M. Breitling, *Macromolecules*, **5**, 279 (1972).
- (5) A. Zambelli, L. Zetta, C. Sacchi, and C. Wolfsgruber, *Macromolecules*, **5**, 440 (1972).
- (6) U. W. Suter and P. J. Flory, *Macromolecules*, **8**, 765 (1975).
- (7) P. J. Flory, "Statistical Mechanics of Chain Molecules", Interscience, New York, 1969.
- (8) G. J. Szasz, N. Sheppard, and D. H. Rank, *J. Chem. Phys.*, **16**, 704 (1948).
- (9) G. Allegra, P. Ganis, and P. Corradini, *Makromol. Chem.*, **61**, 225 (1963).
- (10) R. A. Scott and H. A. Scheraga, *J. Chem. Phys.*, **42**, 2209 (1965).
- (11) G. Allegra, E. Benedetti, and C. Pedone, *Macromolecules*, **3**, 727 (1970).
- (12) It should be noted that  $\varphi_{2i}$ , e.g., expresses both the value of the rotation angle and the skeletal bond ( $2i$ ) around which it is effected.
- (13) (a) A. A. Bothner-By and C. Naar-Colin, *Ann. N.Y. Acad. Sci.*, **70**, 833 (1968); (b) D. R. Ferro, F. Heatley, and A. Zambelli, *Macromolecules*, **7**, 480 (1974); (c) M. Karplus, *J. Chem. Phys.*, **30**, 11 (1959).
- (14) A. Tonelli, private communication.
- (15) A. Zambelli, "NMR—Basic Principles and Progress", Vol. 4, Springer-Verlag, Berlin, Heidelberg, and New York, 1971, pp 101–105.
- (16) P. Corradini, P. Ganis, and P. Oliverio, *Rend. Acc. Naz. Lincei*, **33**, 320 (1962).
- (17) G. Natta, I. Pasquon, P. Corradini, M. Peraldo, M. Pegoraro, and A. Zambelli, *Rend. Acc. Naz. Lincei*, **28**, 539 (1960).
- (18) G. Natta, M. Peraldo, and G. Allegra, *Makromol. Chem.*, **75**, 215 (1964).